Journal of Operation and Automation in Power Engineering
Vol. 2, No. 2, Summer & Fall 2014, Pages:103-112
http://joape.uma.ac.ir

Performance Scrutiny of Two Control Schemes Based on DSM and HB in Active Power Filter

R. Kazemzadeh[1,*], E. Najafi Aghdam[1], M. Fallah[1], Y. Hashemi[2]

[1]Renewable Energy Research Center, Faculty of Electrical Engineering, Sahand University of Technology, Tabriz, Iran

[2]Department of Electrical Engineering, University of Mohaghegh Ardabili, Ardabil, Iran

ABSTRACT

This paper presents a comparative analysis between two current control strategies, constant source power and generalized Fryze current, used in Active Power Filter (APF) applications having three different modulation methods. The Hysteresis Band (HB) and first-order Delta-Sigma Modulation (DSM) as well as the second-order DSM is applied. The power section of the active power filter is viewed as an Analogue to Digital Converter (ADC), then as a result a three-phase shunt active filter modulator controller which, uses Delta-Sigma analogue to digital converter is presented to improve modulator performance. As a result, using second-order Delta-Sigma modulator makes low switching rate compared with first-order Delta-Sigma and hysteresis modulators under same sampling frequency. So, applying this modulator increases system efficiency and reduces cost of switches. In addition, simulation results on MATLAB software show that by using the Delta-Sigma modulator, Total Harmonic Distortion (THD) can be significantly decreased. Moreover, active filter based on the second-order DSM with constant source power has high efficiency and provides lower source current THD.

KEYWORDS: Active power filter, Constant source power, Delta-Sigma modulation, Generalized Fryze current, Hysteresis band.

1. INTRODUCTION

For many years, shunt active power filter has been developed to suppress the harmonics caused by nonlinear loads as well as to compensate the reactive power. The shunt type active power filter eliminates the reactive power and harmonic currents from the grid current by injecting compensation currents intended to result in sinusoidal grid current [1].

The control strategy for a shunt active filter (as shown in Fig. 1) generates the reference current, i_{cref}, that must be provided by the power filter to compensate reactive power and harmonic currents demanded by the load. This involves a set of currents in the phase domain, which should track switching signal applied to the electronic converter by means of the appropriate closed-loop switching control technique such as hysteresis control or dead-beat control [2, 3]. The performance of an active filter mainly depends on the reference current generation strategy. Several papers have studied and compared the performances of different reference current generation strategies under balanced sinusoidal, unbalanced or distorted Alternating Currents (AC) and voltage conditions [4-7].

In general, the shunt active filter consists of two distinct main blocks: (1) active filter controller, and (2) power converter. The controller is responsible for determining the instantaneous compensating reference current, which is continually passed to the power converter. The power converter is responsible for synthesizing the compensating current that should be drawn from the power system by utilizing an adequate modulation method. The power converter should have a high switching frequency

Received: 20 Jan. 2014 Revised: 22 Jun. 2014
Accepted: 07 Jul. 2014
*Corresponding author:
R. Kazemzadeh (E-mail: r.kazemzadeh@sut.ac.ir)

(f_s) in order to reproduce accurately the compensating current. Usually, we have $f_s>10f_{hmax}$, where f_{hmax} represents the frequency of the highest order of harmonic current that must be compensated. Hysteresis control is a well-known current control technique used in voltage-fed PWM converters that forms a non-linear feedback loop. Its advantages are simplicity, outstanding robustness, lack of tracking error, independence of load parameter changes and good dynamics. The hysteresis control drawbacks are needed to extra and variable switching rate, uncontrolled frequency and higher noise compared with other techniques [8, 9]. High switching frequency leads to increasing switching losses and imperfections. Moreover, higher noise causes incorrect performance. Therefore, in this paper, to solve these drawbacks and reducing the THD amount of compensated current (increasing precision of compensation), Delta-Sigma modulation is suggested. Since DSM is an example of pulse-density modulation, the switching pulse waveform can be configured without calculation the on/off time duration. This means that the output switching frequency can be randomly varied under the constant sampling frequency. In addition, DSM has the advantage of harmonic-spreading affects, and pushes off the low-frequency noise [10].

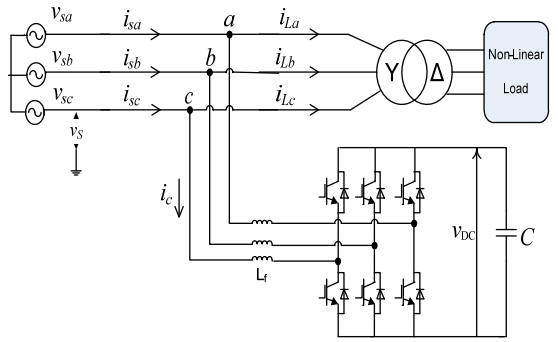

Fig. 1. Shunt active power filter

For this reason, DSM recently has been used for converter in [11-13]. In sections II and III, a review of two control strategies (constant source power and generalized Fryze current) for the extraction of the reference currents is presented. Section IV describes Delta-Sigma modulation and its performance by applying the first and second order loop filters in an active filter. Then, the power section of the active power filter is viewed as an analogue to digital converter, and as a result a three-phase shunt active filter modulator controller which uses Delta-Sigma analogue to digital converter is presented. The remainder of the paper presents comparison of these control strategies using simulation in MATLAB software. The results show that using the first and second order DSM based strategies decreases THD. Moreover, constant source power based on the second-order DSM provides the lowest THD.

2. CONSTANT SOURCE POWER CONTROL STRATEGY

Several methods have been proposed to identify harmonic current such as the methods based on the FFT in frequency domain and the methods based on instantaneous power calculation in time domain. The instantaneous power theory, known as p-q theory, has been developed for three-phase three-wire systems with balanced and sinusoidal source voltage. The compensation target is assumed to get a constant instantaneous source power [14]. This process is shown in Fig. 2. It is based on coordinate transformation from the phase reference system (*abc*) to the *αβ*. The transformation matrix is associated as follows:

$$\begin{bmatrix} v_\alpha \\ v_\beta \end{bmatrix} = \sqrt{\frac{2}{3}} \begin{bmatrix} 1 & -\frac{1}{2} & -\frac{1}{2} \\ 0 & \frac{\sqrt{3}}{2} & -\frac{\sqrt{3}}{2} \end{bmatrix} \begin{bmatrix} v_a \\ v_b \\ v_c \end{bmatrix} \quad (1)$$

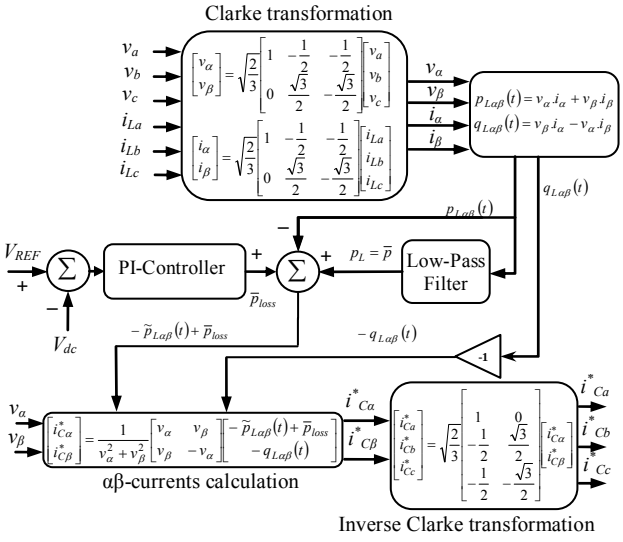

Fig. 2. Block diagram of the constant source power control strategy

$$\begin{bmatrix} i_\alpha \\ i_\beta \end{bmatrix} = \sqrt{\frac{2}{3}} \begin{bmatrix} 1 & -\frac{1}{2} & -\frac{1}{2} \\ 0 & \frac{\sqrt{3}}{2} & -\frac{\sqrt{3}}{2} \end{bmatrix} \begin{bmatrix} i_{La} \\ i_{Lb} \\ i_{Lc} \end{bmatrix} \quad (2)$$

The different power terms are defined as follows:

$$\begin{bmatrix} p_{L\alpha\beta}(t) \\ q_{L\alpha\beta}(t) \end{bmatrix} = \begin{bmatrix} v_\alpha & v_\beta \\ -v_\beta & v_\alpha \end{bmatrix} \begin{bmatrix} i_\alpha \\ i_\beta \end{bmatrix} = [T] \begin{bmatrix} i_\alpha \\ i_\beta \end{bmatrix} \quad (3)$$

Considering inverse matrix [T], it is possible to calculate the current components by means of the different power terms. The expression is given in the next equation:

$$\begin{bmatrix} i_\alpha \\ i_\beta \end{bmatrix} = \frac{1}{v_{\alpha\beta}^2} \begin{bmatrix} v_\alpha & -v_\beta \\ v_\beta & v_\alpha \end{bmatrix} \begin{bmatrix} p \\ q \end{bmatrix} \quad (4)$$

where, $v_{\alpha\beta}^2 = v_\alpha^2 + v_\beta^2$, p is the $\alpha\beta$ real instantaneous power, and q is the imaginary instantaneous power.

The strategy assumed in this theory has been obtained using a constant instantaneous power as the source side with the only restriction of getting a null average instantaneous power exchanged by the compensator *pc*.

In order to calculate the compensator current, it is verified that:

$$p_c(t) = p_L(t) - p_s(t) = p_L(t) - p_L \quad (5)$$

wherep_L is the total active power incoming to the load. Equation (5) can be expressed in the following way:

$$p_{c\alpha\beta}(t) = p_{L\alpha\beta}(t) - p_{\alpha\beta} = \tilde{p}_{L\alpha\beta}(t) \quad (6)$$

Which, effectively, fulfils the average value becomes zero as $\langle p_c(t) \rangle = 0$, where $\tilde{p}_L(t)$ represents the AC part of the $p_L(t)$. On the other hand, the instantaneous imaginary power exchanged by the compensator must be the same as the instantaneous imaginary power required by the load: $q_c(t) = q_{L\alpha\beta}(t)$.

3. GENERALIZED FRYZE CURRENT CONTROL STRATEGY

The fundamentals of the *pq* theory are exploited to develop a control strategy, the generalized Fryze current control based on the minimization method of equation [15, 16]. The number of equations is reduced since it does not utilize any reference frame transformation. The control strategy for a shunt active filter that has denominated as the generalized Fryze currents is shown in Fig. 3. The product between the phase voltages v_a, v_b, v_c and load currents i_{La}, i_{Lb} and i_{Lc} will determine the instantaneous active three-phase power of the load. At the same time, the square sum of phase voltages (v_a, v_b, v_c) is determined.

The conductance G_e is determined by the division between the active three-phase power and squared instantaneous aggregate voltage (v_a, v_b, v_c). This conductance comprises all current components that produce active power with voltages v_a, v_b and v_c.

A low-pass filter will extract the average value of the conductance $\overline{G}_e$. The DC voltage regulator control circuit determines the signal $\overline{G}_{loss}$. Control signal, $\overline{G}_e + \overline{G}_{loss}$ with the control voltages v_a, v_b and v_c which are used to determine the active current are pure sinusoidal waves in phase with v_a, v_b and v_c include only the portion (proportional $\overline{G}_e$) of load current that produces active power, and the active current (proportional to G_{loss}) that is necessary for losses compensation in the shunt active filter. Since the shunt active filter compensates the difference between the calculated active current and measured load current, it is possible to guarantee that the source currents i_{as}, i_{bs} and i_{cs} drawn from the network are always sinusoidal, balanced and in phase with positive-sequence voltages. The DC voltage regulator is used to generate control signal $\overline{G}_{loss}$ as shown in Fig. 3. This signal forces the shunt active filter to drawn an additional active current from the network to compensate losses in the power circuit of the shunt active filter. Additionally, it corrects DC voltage variations caused by abnormal operation and transient compensation errors. It consists only of a closed loop PI-controller [$G(s) = k_p + \frac{k_i}{s}$].

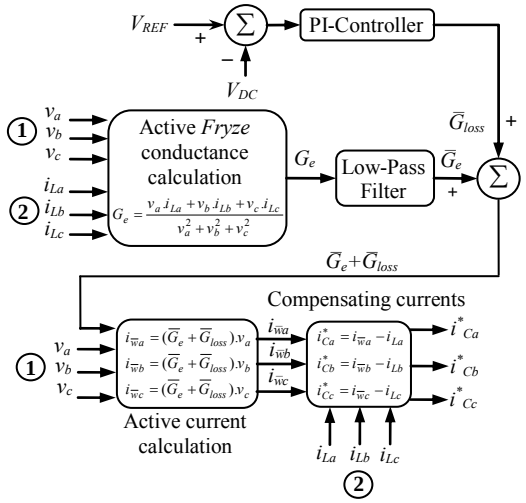

Fig. 3. Block diagram of the generalized Fryze current control strategy

4. DELTA-SIGMA MODULATION IN POWER ELECTRIC APPLICATIONS

In the proposed switching power converter, an analogue to digital (A/D) converter is used to properly prepare the state of switches. In other words, the analogue input is the compensating current reference signal to be synthesized, and the quantized digital output is the state of the circuit switches.

A/D conversion is an inherent non-linear operation and introduces errors to the conversion (known as quantization noise) [17]. In both communications and power electronics implementations, the purpose is to design the system so that the input signal is passed through the system with minimal distortion from noise.

Oversampling Delta-Sigma technique is one of the best quantization noise reduction methods [18]. This modulator does not reduce the magnitude of the quantization noise, but instead, shapes the noise. It shapes power density spectrum of noise by moving the energy toward higher frequencies and reducing quantization noise within the signal band as depicted in Fig. 4 [10, 18]. Increased noise in the high frequency band can be removed by using a simple low pass filter. In fact, Delta-Sigma modulators achieve better conversion performance by using a low-resolution quantizer in a feedback loop with linear filtering [19]. The quantizer can be modeled using an input-independent additive white noise [20], which is very simple and useful for many practical purposes. Fig. 5 shows the structure of Delta-Sigma modulator [10].

Since power switching converters typically switch at frequencies well in excess of the input Nyquist rate, the Delta-Sigma modulation technique can be employed in power electronics application as the cases [21].

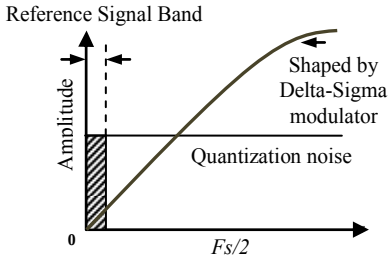

Fig. 4. The Delta-Sigma modulator noise-shaping characteristic (first-order)

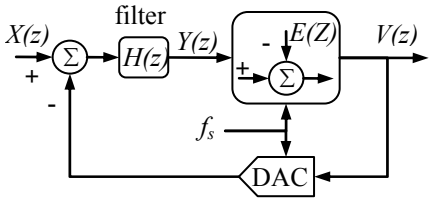

Fig. 5. Block diagram of Delta-Sigma modulator

To illustrate how a power electronic circuit can be embedded in a Delta-Sigma modulator, consider the modulator for the half-bridge converter shown in Fig. 6. In this arrangement, the gating circuitry and half-bridge are embedded into the loop following the latch. The comparator and latch set the switch state for each sampling period according to the sign of the comparator input at the sampling instant. The switch state impresses the voltage at the output. Thus, taking the input signal to be the desired output voltage, the actual output voltages can follow the desired state. Output passive low pass filter exists in the APF's inverter serves as a converter on the feedback path which transforms two level output voltage of the inverter to continuous current that follows reference signal. In addition, the nature of the low pass transfer function in the APF's inverter acts the role of a decimation filter. In other words, the passive filter in active shunt filter structure, serves as a digital to analogue (D/A) converter mentioned in Fig. 4, as well as filtering out of band quantization noise shaped towards high frequencies.

A typical input-output transfer characteristic of a monobit quantizer is a stair function. Obviously, an infinite number of input amplitudes can be mapped to a unique output level resulting in loss of exact information of the input magnitude and hence impose the quantization error (*E(z)*). Based on the Bennette's method for approximating quantization function [22], the quantizer can be linearized using an input-independent additive white noise model in order to make the analysis tractable. Under such an approximation, the nonlinear modulator becomes a linear system with a stochastic input, and the performance can be easily derived in *Z* domain.

$$V(z) = STF(z)X(z) + NTF(z)E(z) \quad (7)$$

$$STF(z) = \frac{V(z)}{X(z)} = \frac{H(z)}{1+H(z)} = z^{-L} \quad (8)$$

$$NTF(z)\frac{V(z)}{E(z)} = \frac{1}{1+H(z)} = (1-z^{-1})^{L} \quad (9)$$

The first order Delta-Sigma modulator is the simplest structure; where $H(z)= z\text{-}1/1\text{-}z^{-1}$ is discrete mode or equivalent *1/s* in continuous-time type of modulator [22].

A way to further noise reduction is to use a higher order Delta-Sigma modulator. A second-order continuous time Delta-Sigma modulator is shown in Fig. 6 (b), where, a first-order modulator is embedded in the second loop with an integrator in the feed-forward path. Compared with the first-order modulator, the second-order modulator has one more design parameter available; it is the ratio of the gains of two paths; this makes it capable to determine low frequency properties of the circuit by outer path and improve system stabilizing while determining high frequency properties by inner path. Moreover, by a deliberate increase in the inner loop, delay in the outer loop can be compensated [18].

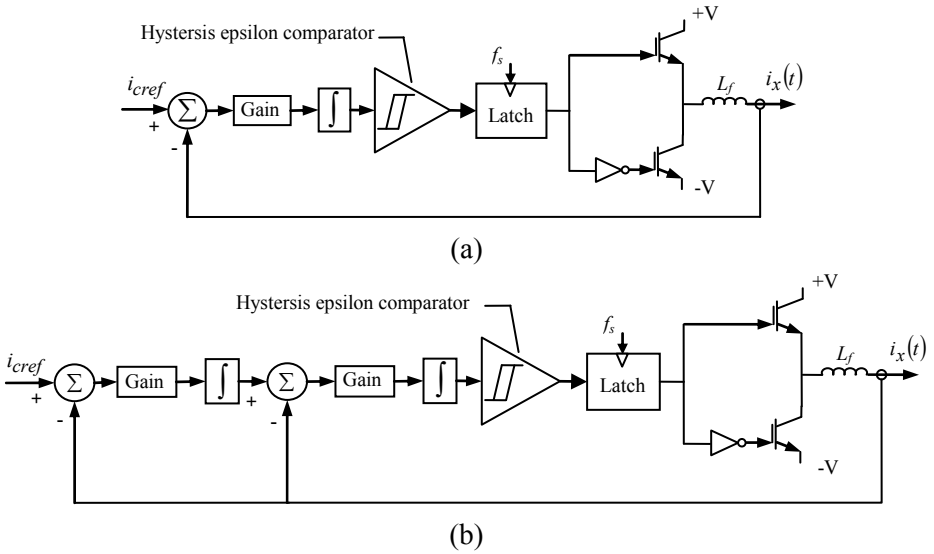

Fig. 6. Half-bridge embedded in Delta-Sigma modulator loop; a) first-order, b) second-order

Higher order modulators also are possible to construct, but they cannot simply be made by adding further stages as above. The reason is that the phase shift caused by more than two integrators will make the system unstable [18].

The first statement of (7) presents Signal Transfer Function (STF), and the second statement shows Noise Transfer Function (NTF). STF is generally flat in the band for the first and second order modulators, however the difference between first, second and third order modulator can affect differently on the modulator's performance.

The NTF of systems is shown in Fig. 7. Regarding to comparison of STF and NTF, and having stability problem, system complexity and implementation problems of the modulators of orders higher than 2 in view, it becomes manifest that a second-order Delta-Sigma modulator is a better compromise between circuit complexity and signal to noise ratio. Therefore, a second order Delta-Sigma modulator is chosen for emerging in the proposed active power filter.

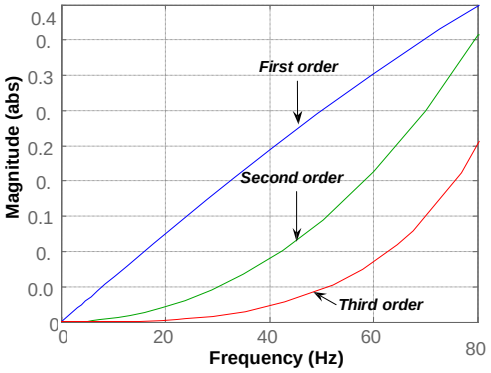

Fig. 7. Magnitude spectra for NTFs

Since, the proposed modulator will be implemented using continuous time integrator, once the order of modulator is chosen (second order here as depicted in Fig. 6(b)), it is usually designed in discrete or *Z* domain then, transferred to continuous time domain using the following equation as impulse-invariant transform method [10]:

$$Z^{-1}\{H(z)\} = L^{-1}\{R_D(s) \cdot H(s)\}_{t=nTs} \quad (10)$$

where *H(s)* is equivalent Laplace transform of *H(z)* together with *RD(s)* which is the impulse response of the DAC on the feedback path. In the simplest second order modulator case, discrete to continuous time conversion results in the structure are shown in Fig.8, where all zeros of the selected NTF are non-optimized and laid at real zero.

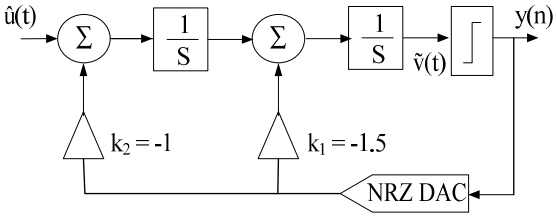

Fig. 8. Discrete to continuous time conversion of second order modulator

5. SIMULATION RESULTS

The harmonic currents and reactive power compensation by APF is implemented in a three-phase power system which the power system voltage of 380^{V} and thyristor rectifier with three types of resistive-inductive, resistive and inductive (are intended as A, B and C in Table 1, respectively) loads as the harmonic current compensation objects are considered. The design specifications and the circuit parameters used in the simulation are indicated in Table 1.

In the second loop control strategy, a structure of the second-order Delta-Sigma modulator, as mentioned above in the Fig. 6, is used. For the simulation of the active filter operation, it is used a balanced and sinusoidal three-phase voltage system where two different methods to control the active filter are applied. Judging from these results, it is clear that the Delta-Sigma modulator system compared to the HB modulated system has better performance in two different methods to control the active filter in terms of lower THD and better-compensated currents wave shape. Table 2-3 show the general characteristics of both systems in terms of harmonic components. Main AC voltage is illustrated in Fig. 8. In the case of resistive-inductive load, line current is shown in Fig. 9.

Table 1. Parameter values of simulation

Parameter	Parameter value
System voltage	380 V
Load	3-phase thyristor by 20° firing angle rectifier with A) 10 mH- 20 ohm, B) 10 ohm and C)2 H loads, fed by a YΔ transformer
Filter Inductance	0.5 mH
Dc link capacitors	1200 µF
DC link reference voltage	800 V
Sampling frequency	30 kHz

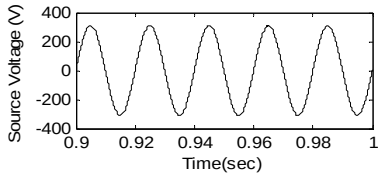

Fig. 9. Balanced and sinusoidal voltage

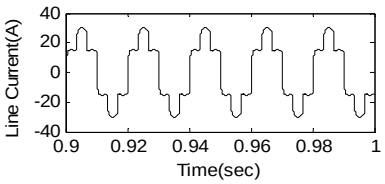

Fig. 10. Line current waveform of resistive-inductive load

Compensated line current and filter current in case of resistive-inductive load by the constant source power and the generalized Fryze current control strategies for HB, first-order Delta-Sigma and

second-order Delta-Sigma modulation systems are illustrated in Figs. 10-13.

In the cases of pure resistive and inductive loads, line current is depicted in Fig. 14. Also, compensated line current of pure resistive and inductive loads by mentioned control strategies with different modulations are shown in Figs. 15-16 and Figs. 17-18, respectively. Note that simulations are made for a three-phase system, but only one phase (phase A) is shown in figures to make images clear to present avoidance of visual error.

Finally, general characteristics of load harmonics and compensated current with three types of modulation systems for pure resistive and inductive loads are presented in Tables 4-5 and 6-7, respectively.

Another advantage of Delta-Sigma modulation in comparison with hysteresis modulation is the lower switching rate under the same sampling frequency. The benefits of low switching of Delta-Sigma modulation technique are low switching losses, imperfection and cost. Thus, reducing the switching losses will increase the system efficiency. A comparison of relative switching losses in the power circuit of the shunt active power filter by the constant source power control strategy with three types of modulation is summarized in Table 8.

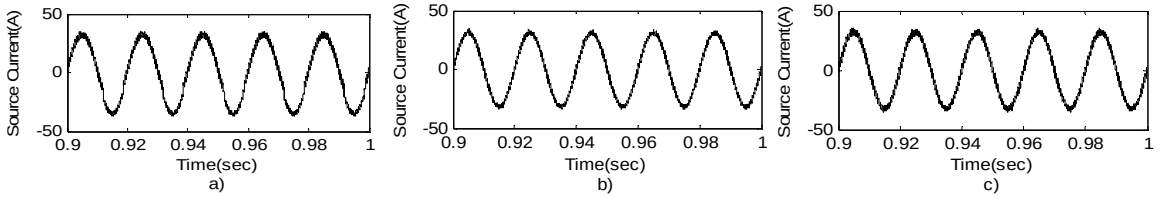

Fig. 11. Compensated currents by the constant source power control strategy using (a) HB, (b) First-order Delta-Sigma (c) Second-order Delta-Sigma modulation

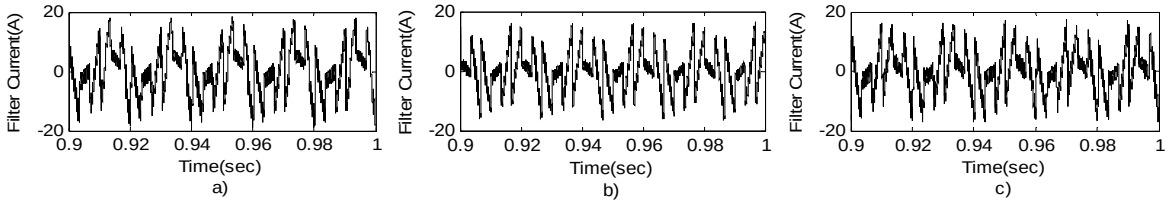

Fig. 12. APF currents by the constant source power control strategy using (a) HB (b) First-order Delta-Sigma (c) Second-order Delta-Sigma modulation

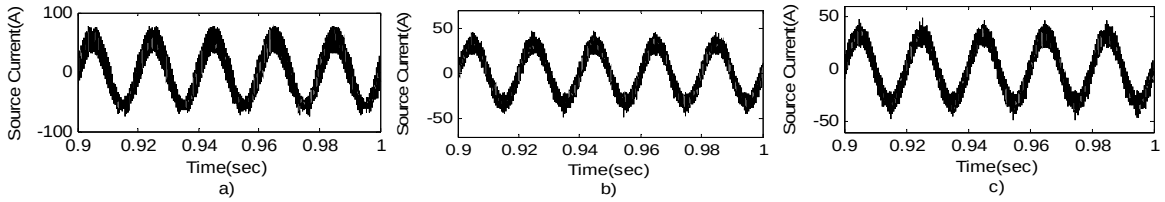

Fig. 13. Compensated currents by the generalized Fryze current control strategy using (a) HB (b) First-order Delta-Sigma (c) Second-order Delta-Sigma modulation

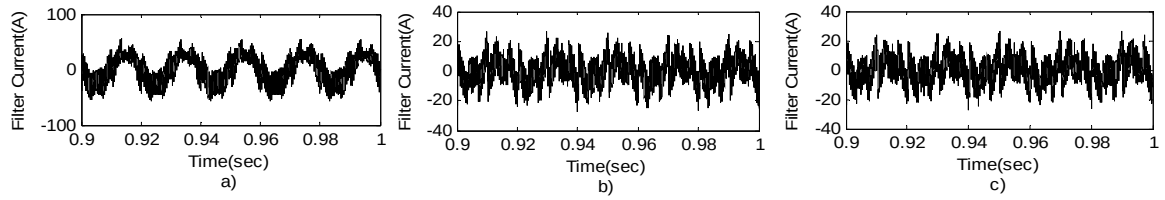

Fig. 14. APF currents by the generalized Fryze current control strategy using (a) HB (b) First-order Delta-Sigma (c) Second-order Delta-Sigma modulation

Table 2. Harmonic componets demanded to AC mains by resistive-inductive load wihout APF and with mentiond APFs by the constant source power control strategy

	Without APF	HB controlled APF	First delta-sigma controlled APF	Second delta-sigma controlled APF
I_3	0.00%	0.01%	0.01%	0.01%
I_5	21.81%	1.71%	0.34%	0.11%
I_7	11.61%	1.26%	0.48%	0.22%
I_9	0.00%	0.02%	0.03%	0.04%
I_{11}	8.37%	0.73%	0.10%	0.09%
I_{13}	6.22%	0.78%	0.09%	0.13%
I_{15}	0.00%	0.03%	0.02%	0.01%
I_{17}	4.81%	0.46%	0.04%	0.11%
I_{19}	3.92%	0.48%	0.18%	0.12%
THD	28.06%	7.74%	1.94%	1.68%

Table 3. Harmonic componets demanded to AC mains by resistive-inductive load wihout APF and with mentiond APFs by the generalized Fryze current control strategy

	Without APF	HB controlled APF	First delta-sigma controlled APF	Second delta-sigma controlled APF
I_3	0.00%	0.14%	0.16%	0.08%
I_5	21.81%	3.24%	2.95%	2.72%
I_7	11.61%	0.83%	0.68%	0.63%
I_9	0.00%	0.12%	0.10%	0.13%
I_{11}	8.37%	1.31%	0.16%	0.22%
I_{13}	6.22%	1.16%	0.63%	0.68%
I_{15}	0.00%	0.31%	0.02%	0.07%
I_{17}	4.81%	0.41%	0.62%	0.25%
I_{19}	3.92%	0.47%	0.79%	0.48%
THD	28.06%	12.58%	7.43%	6.83%

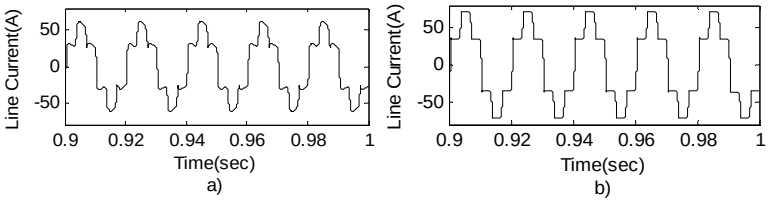

Fig. 15. Line current waveform of pure (a) resistive load, (b) inductive load

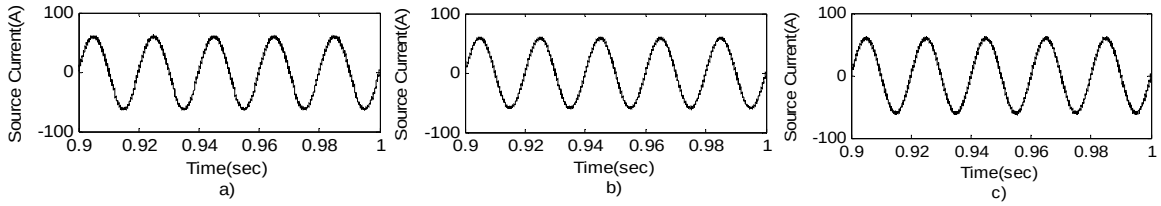

Fig. 16. Compensated currents by the constant source power control strategy using (a) HB, (b) First-order Delta-Sigma (c) Second-order Delta-Sigma modulation

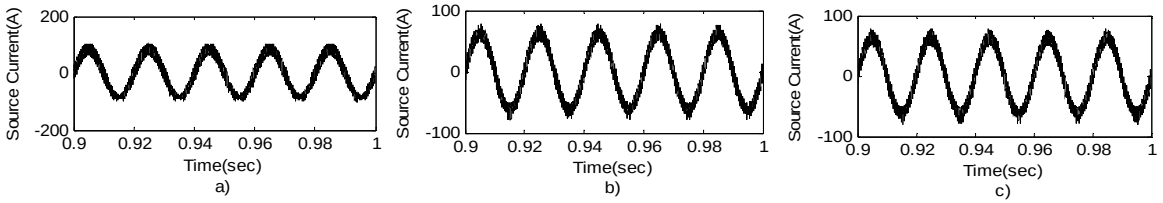

Fig. 17. Compensated currents by the generalized Fryze current control strategy using (a) HB (b) First-order Delta-Sigma (c) Second-order Delta-Sigma modulation

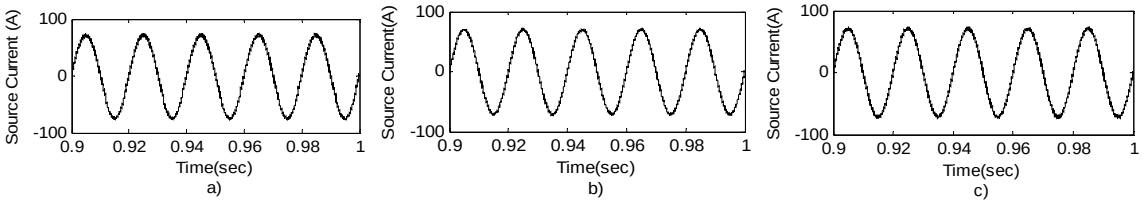

Fig. 18. Compensated currents by the constant source power control strategy using (a) HB, (b) First-order Delta-Sigma (c) Second-order Delta-Sigma modulation

6. CONCLUSION

This paper has provided a comparative analysis of two control strategies and three modulation techniques for shunt APF. For instance, in constant source power and generalized Fryze current control strategies, using a first-order DSM results in lower

line current distortion when compared to HB modulation. Furthermore, for the same conditions, using the second-order DSM guarantees better performance than that of the first-order DSM. Based on theoretical discussion and simulation results, it can be concluded that the use of DSM instead of HB increases the compensation accuracy and reduces switching losses. In addition, under same sampling frequency, switching frequency of Delta-Sigma modulation and therefore its switching losses is lower than HB modulation. Also, among mentioned methods, the performance of the constant source power control strategy compared with the generalized Fryze current control strategy is better. Thus, based on our comparative analysis, constant source power control strategy with second DSM can be proposed as the best control structure for shunt active filter.

Table 4. Harmonic componets demanded to AC mains by pure resistive load wihout APF and with mentiond APFs by the constant source power control strategy

	Without APF	HB controlled APF	First delta-sigma controlled APF	Second delta-sigma controlled APF
I_3	0.00%	0.03%	0.01%	0.04%
I_5	22.59%	0.94%	0.15%	0.08%
I_7	10.46%	0.68%	0.20%	0.20%
I_9	0.00%	0.04%	0.03%	0.04%
I_{11}	8.25%	0.48%	0.20%	0.18%
I_{13}	5.08%	0.48%	0.07%	0.04%
I_{15}	0.00%	0.02%	0.03%	0.02%
I_{17}	4.30%	0.24%	0.18%	0.16%
I_{19}	2.78%	0.20%	0.05%	0.09%
THD	27.44%	4.31%	1.08%	0.97%

Table 5. Harmonic componets demanded to AC mains by pure resistive load wihout APF and with mentiond APFs by the generalized Fryze current control strategy

	Without APF	HB controlled APF	First delta-sigma controlled APF	Second delta-sigma controlled APF
I_3	0.00%	0.12%	0.03%	0.07%
I_5	22.59%	1.87%	2.31%	2.15%
I_7	10.46%	0.48%	0.71%	0.71%
I_9	0.00%	0.02%	0.05%	0.07%
I_{11}	8.25%	0.05%	0.02%	0.03%
I_{13}	5.08%	0.65%	0.38%	0.35%
I_{15}	0.00%	0.04%	0.05%	0.04%
I_{17}	4.30%	0.40%	0.38%	0.31%
I_{19}	2.78%	0.16%	0.15%	0.14%
THD	27.44%	6.66%	5.04%	4.68%

Table 6. Harmonic componets demanded to AC mains by pure inductive load wihout APF and with mentiond APFs by the constant source power control strategy

	Without APF	HB controlled APF	First delta-sigma controlled APF	Second delta-sigma controlled APF
I_3	0.00%	0.03%	0.02%	0.02%
I_5	19.47%	0.93%	0.08%	0.06%
I_7	13.53%	0.71%	0.25%	0.20%
I_9	0.00%	0.02%	0.02%	0.02%
I_{11}	7.92%	0.46%	0.07%	0.10%
I_{13}	6.34%	0.50%	0.12%	0.11%
I_{15}	0.00%	0.00%	0.02%	0.01%
I_{17}	4.21%	0.24%	0.08%	0.09%
I_{19}	3.45%	0.18%	0.09%	0.08%
THD	26.63%	4.37%	1.08%	0.94%

Table 7. Harmonic componets demanded to AC mains by pure inductive load wihout APF and with mentiond APFs by the generalized Fryze current control strategy

	Without APF	HB controlled APF	First delta-sigma controlled APF	Second delta-sigma controlled APF
I_3	0.00%	0.09%	0.04%	0.14%
I_5	19.47%	1.89%	2.27%	1.55%
I_7	13.53%	0.39%	0.75%	0.17%
I_9	0.00%	0.02%	0.08%	0.08%
I_{11}	7.92%	0.10%	0.10%	0.14%
I_{13}	6.34%	0.58%	0.37%	0.35%
I_{15}	0.00%	0.10%	0.01%	0.15%
I_{17}	4.21%	0.35%	0.39%	0.20%
I_{19}	3.45%	0.17%	0.22%	0.53%
THD	26.63%	6.32%	4.66%	4.29%

Table 8. Comparison of relative switching losses

APF Control Strategy	Constant source power		
Modulation	Hysteresis	First-Order DS	Second-Order DS
Relative Losses	1	0.97	0.93

REFERENCES

[1] H.R. Imanijajarmi, A. Mohamed, H. Shareef, , "Active power filter design by a novel approach of multi-objective optimization", *Journal of Operation and Automation in Power Engineering*, vol. 1, no. 1, pp. 54-62, 2013.

[2] Y. Han, L. Xu, G. Yao, L. Zhou, M. Khan and C. Chen, "A robust deadbeat control scheme for active power filter with LCL input filter," *Electrical Review,* vol. 86, no. 2, pp. 14-19, 2010.

[3] Y. He, J. Liu, J. Tang, Z. Wang and Y. Zou, "Deadbeat control with a repetitive predictor for three-level active power filters," *Journal of Power Electronics,* vol. 11, no. 4, pp. 583-590, 2011.

[4] G.W. Chang and T.C. Shee, "A novel reference

compensation current strategy for shunt active power filter control" *IEEE Transactions on Power Delivery*, vol. 19, no. 4, pp. 1751-1758, 2004.

[5] G.W. Chang and C.M. Yeh, "Optimization-based strategy for shunt active power filter control under non-ideal supply voltages," *IEE Proceedings on Electric Power Applications,* vol. 152, no. 2, pp. 182-190, 2005.

[6] K.S. Hong and C.S. Kim, "A DSP based optimal algorithm for shunt active filter under non-sinusoidal supply and unbalanced load conditions," *IEEE Transactions on Power Electronics*, vol. 22, no. 2, pp. 593-601, 2007.

[7] M.I.M. Montero, E.R. Cadaval and F.B. Gonzalez, "Comparison of control strategies for shunt active power filters in three-phase four-wire systems," *IEEE Transactions on Power Electronics*, vol. 22, no. 1, pp. 229-236, 2007.

[8] A. M. Razali, M. A. Rahman and N. A. Rahim, "An analysis of current control method for grid connected front-end three phase AC-DC converter," *Proceedings of the IEEE ECCE Asia Downunder Conference,* pp. 45-51, 2013.

[9] C. Attaianese, M. Di Monaco and G. Tomasso, "High performance digital hysteresis control for single source cascaded inverter," *IEEE Transactions on Industrial Informatics,* vol. 9, no. 2, pp. 620-629, 2013.

[10] P.M. Aziz, H.V. Sorensen and J. Vn der Spiegel, "An overview of sigma-delta converters," *IEEE Signal Processing Magazine,* vol. 13, no. 1, pp. 61-84, 1996.

[11] Y. Wang, and D. Ma, "Design of Integrated Dual-Loop Delta–Sigma Modulated Switching Power Converter for Adaptive Wireless Powering in Biomedical Implants" *IEEE Transactions on Industrial Electronics,* vol. 58, no. 9, pp. 4241-4249, 2011.

[12] J. Paramesh and A. Von iouanne, "Use of sigma-delta modulation to control EMI from switch-mode power supplies," *IEEE Transactions on Industrial Electronics*, vol. 48, no. 1, pp. 111-117, 2001.

[13] J. Amini, R. Kazemzahed, H. Madadi Kojabadi, "Performance enhancement of indirect matrix converter based variable speed Doubly-Fed induction generator", *Proceedings of the 1st Conferenceon Power Electronic & Drive Systems & Technologies*, pp. 450-455, 2010.

[14] M. Popescu, A. Bitoleanu and V. Suru, "A DSP-Based implementation of the p-q theory in active power filtering under nonideal voltage conditions," *IEEE Transactions on Industrial Informatics*, vol. 9, no. 2, pp. 880-889, 2013.

[15] M. Aredes, L.F.C. Monteiro and J. Mourente, "Control strategies for series and shunt active filters," *Proceedings of the IEEE Power Technology Conference*, vol. 2, 2003.

[16] A.E. Leon, S.J. Amodeo, J.A. Solsona and M. I. Valla, "Non-linear optimal controller for unified power quality conditioners," *IET Power Electronics,* vol. 4, no. 4, pp. 435-446, 2011.

[17] L.F.C. Monteiro and M. Aredes, "A compare-ative analysis among different control strategies for shunt active filters," *Proceedings of the Industrials Applications Conference,* pp. 345-350, 2002.

[18] S.R. Norsworthy, R. Schreier and G.C. Temes, "Delta-Sigma data converters-theory, design, and simulation," *IEEE Press*, 1997.

[19] E.N. Aghdam, "Nouvelles techniques d'appariement dynamique dans un CNA multibit pour les convertisseurs sigma-delta," Doctoral Dissertation," *University of Paris*, 2006.

[20] W. R. Bennett, "Spectra of quantized signals," *Bell System Technical Journal,* vol. 27, no. 3, pp. 446-472, 1948.

[21] E. Monmasson, "Power Electronic Converters," *France, Wily*, 2009.

[22] L. Breems and J.H. Huijsing, "Continuous- time sigma-delta modulation for A/D conversion in radio receivers," *Springer*, 2001.